IEEE Access
Multidisciplinary ⋮ Rapid Review ⋮ Open Access Journal

Received 8 July 2023, accepted 14 August 2023, date of publication 18 August 2023, date of current version 25 August 2023.

Digital Object Identifier 10.1109/ACCESS.2023.3306409

RESEARCH ARTICLE

Two-Level Optimal Bidding Strategy for Load Aggregator Based on a Data-Driven Approach Combined With LSTM-Based Forecasting and Agent-Based Models

HAN SEOK RYU*, HYUNG JOON KIM*, AND MUN KYEOM KIM
Department of Energy System Engineering, Chung-Ang University, Dongjak, Seoul 06974, Republic of Korea

Corresponding author: Mun Kyeom Kim (mkim@cau.ac.kr)

This work was supported in part by the Chung-Ang University Research Grant in 2022, and in part by the Basic Science Research Program through the National Research Foundation of Korea (NRF) funded by the Ministry of Education under Grant 2020R1A2C1004743.

*Han Seok Ryu and Hyung Joon Kim are co-first authors.

ABSTRACT Demand response (DR) is an economical way of addressing the challenges faced by the massive penetration of distributed energy resources, such as renewable energy. Residential consumers account for a significant proportion of electricity consumption. However, their behavior is highly random and uncertain, meaning it is difficult to quantify the impact of DR programs in which they participate. This paper presents a two-level optimal bidding strategy framework for load aggregators that combines a data-driven forecasting model and a data-driven agent-based model (D-ABM) to provide a realistic estimate of the impact of DR. First, the aggregated load of all consumers and market prices are predicted via a long short-term memory (LSTM) autoencoder forecasting model. Then, the proposed D-ABM estimates and quantifies the difference rate in terms of total load due to DR. Since D-ABM is a bottom-up approach, each consumer can be treated as a heterogeneous agent and changes in individual electricity usage patterns due to DR can be estimated. Changes in collective electricity consumption patterns can also be quantified by considering the estimated individual behavior and the interactions defined by the basic rules. In addition, assumptions about biases and preferences that explain the irrationality of individual decision-making are given to agents, and the uncertainty of DR participation is considered more realistically. Finally, based on these uncertainties addressed at each level, various bidding strategies for load aggregators can be obtained. The numerical simulation results indicate that our framework provides a more realistic estimation of the impact of total load under DR, minimizes any deviations from bidding strategies, and ensures maximum profits for load aggregators.

INDEX TERMS Bidding strategy, load aggregator, demand response, long short-term memory autoencoder, data-driven agent-based model.

I. INTRODUCTION

A. MOTIVATION

Demand response (DR) programs trigger changes in end-user consumption patterns in response to market price signals. As a flexible demand-side resource, DR is considered an efficient tool for maintaining the reliability of power systems and solving the problem of the massive penetration of distributed energy resources, such as renewable generation. Residential consumers account for a significant proportion of electricity consumption among all end-users and present a significant opportunity for implementing DR programs. However, designing an efficient DR mechanism for the residential sector presents significant challenges due to the large number of consumers and their negligible individual impact on the market [1]. Given these limitations, load aggregators

The associate editor coordinating the review of this manuscript and approving it for publication was Jethro Browell.

have emerged as a means of participating in the wholesale power market on behalf of individual residential consumers. However, this emergence of DR and load aggregators has created new challenges for the entire chain, including market operators, load aggregators, and residential consumers.

Increased participation in DR programs can complicate the power flow in demand-side networks, which affects electricity consumption patterns and load forecasting [2]. For load aggregators, accurately quantifying and estimating the impact of DR program is crucial when submitting bidding strategies in day-ahead markets [3]. In other words, before trading in day-ahead markets, load aggregators need to understand the rate of change in the total load due to DR. However, the behavior of residential consumers is heterogeneous. Therefore, even with similar dwelling sizes, similar occupancy, similar sets of appliances, and identical geographical conditions, their energy consumption can vary by up to 200% [4]. Moreover, sensitivity to DR signals can vary depending on the behavior and lifestyle of the consumer. Thus, load aggregators encounter difficulties when attempting to understand and consider these individual characteristics that determine electricity consumption.

The development of smart meters is transforming power systems into smart power networks, and the received data can provide important clues toward understanding end-user behavior. In other words, immense amounts of granular electricity consumption data can be collected due to the widespread advances in smart meters [5], and this high-resolution data can provide rich information about consumers' electricity consumption patterns and lifestyles. Through data learning and analyses, this abundant data presents an opportunity to objectively quantify and estimate the degree of load change under DR programs. From another perspective, existing studies on DR that assume that end-users are always rational and active economic entities lead to inexplicable gaps between modeling results and actual observations [6]. For example, some price-responsive loads may not consistently change their electricity consumption behavior in response to price signals. Moreover, the degree of change can also differ from the expected value. In particular, in situations where consumers are autonomous, the irrationality of their decision-making must also be considered when estimating the impact of DR. Therefore, this study aims to provide more realistic estimates and quantify changes in total load under DR programs by proposing a data-driven two-level optimal bidding strategy framework. This will allow load aggregators to address various uncertainties related to bidding strategies, including the irrationality of consumer decision making.

B. LITERATURE REVIEW

Residential consumers could theoretically represent a great additional source of flexibility with significant potential for decarbonizing energy systems [7]. Many studies have focused on a variety of topics for effectively implementing DR programs for residential electricity consumers [8]. One of these is the task of forecasting loads affected by the implementation of a DR program. In [9], a load prediction strategy based on a combined approach of artificial neural networks (ANN) and wavelet transform (WT) was proposed to evaluate DR-driven load pattern elasticity in smart households. This approach was employed to predict the response of residential loads to various price signals. In [10], a forecasting model based on a novel support vector regression (SVR) method was proposed to calculate the DR baseline, which took the ambient temperature 2 h before the DR execution as an input variable by exploiting the nonlinear characteristics of SVR.

In [11], a novel stacked autoencoder (SAE)-based residential customers baseline load (CBL) estimation method was presented using the data reconstruction capability of SAE. A support vector machine (SVM) classifier was self-trained for pseudo-load selection, and the results indicated that the accuracy of residential CBL reconstruction was significantly improved.

As the consumer's role in the DR framework is an active participant, the uncertainty of their response should be considered. In [12], a method for predicting consumer response behavior based on long short-term memory (LSTM) was proposed. Since consumer response behavior characteristics are variable and exhibit a strong correlation with the timeline, the characteristics of the LSTM algorithm were analyzed based on the behavior analysis results. In [13], a load forecasting method was developed based on DR deviation correction to reflect the behavior of DR consumers. The process of DR deviation correction consists of the acquisition of the initial deviation sequence, normalization, extraction of the Hankel matrix, and singular value decomposition of the simplified mapping matrix. In [14], a comprehensive market framework was introduced in which consumer agents could deliver proactive residential DR measures in a day-ahead market. Using agent-based modeling and a simulation approach, the difference in DR potential was captured in advance and the residential load profile was modeled by classifying each household type. To estimate practical and realistic DR potentials, [15] proposed a resident behavior detection model for environment-responsive DR potential estimations. This method was based on a hidden Markov model and time-varying Markov chains in which the sub-metering data of appliances were variously analyzed and profiled. Another perspective is to quantify the response of residential consumers according to their degree of comfort. In [16], the DR potential of residential users was comprehensively predicted based on the evaluation criteria of potential load level, use consistency score, and frequency of use. In addition, user comfort was multidimensionally evaluated, and a hybrid DR model that considered the influence of electricity price and economic incentives on the willingness to participate in DR was established. In [17], a bi-level robust optimization model with demand response and thermal comfort was presented that considered the uncertainties of multi-energy loads and renewable energy forecasting. Moreover, robust optimization

of integrated energy systems was performed, with carbon emission value (CEV) and resident dissatisfaction index (RDI) used as the objective functions.

Recently, several studies have considered DR to formulate the bidding strategies of load aggregators. In [18], an optimal bidding strategy model for a load aggregator including DR was proposed that could reduce the risk of financial losses due to price fluctuations. This was addressed as a mixed-integer linear programming problem. In [19], risk-based hybrid energy management of a grid-connected microgrid was presented based on stochastic/information gap decision theory optimization considering the confidence-based incentive DR (CIDR). By implementing a CIDR program with a DR aggregator, the proposed hybrid energy management scheme improved stability during peak period loads, ensuring economical operation of the microgrid. In [20], a game theory-based approach was devised to obtain the best bidding strategy for DR aggregators in the electricity market. This employed an economically responsive load model based on the customer benefit function and price elasticity combined with the DR approach. In [21], a dynamic bidding strategy for demand-side resources was proposed. This allowed DR aggregators to participate in the frequency regulation market considering the risks of various uncertain factors in the electricity market. Moreover, a time-varying compensation method for DR was devised based on analyzing the response potential of demand-side resources, and the bidding strategy of the DR aggregator was dynamically optimized by considering load deviations.

C. CONTRIBUTIONS

Significant advances have been made in recent years on methods that predict user behavior. However, regardless of whether this is an approximate abstract function or a linear or nonlinear approximation, it remains a challenging task to describe the relationship in terms of a time series [12]. The process of addressing price-responsive uncertainties in individual consumers is often too complicated or is only concerned with the comfort related to certain appliances. Moreover, existing studies on bidding strategies of the load aggregator that consider DR have focused mainly on optimization based on operation and compensation mechanisms for DR programs.

Accordingly, this paper proposes a two-level optimal bidding strategy framework that combines an efficient forecasting model and the data-driven agent-based model (D-ABM) to provide realistic estimates of the impact of DR. First, the aggregated loads and market prices are predicted through a long short-term memory (LSTM) autoencoder-based forecasting model using multivariate time-series data. Simultaneously, D-ABM addresses the price-responsive uncertainty of individual consumers in their DR participation and estimates the rate of change in total load due to DR. Finally, considering the associated uncertainties addressed at each level, the load aggregator's bidding strategy is determined, ensuring maximum profit by reducing the deviation between actual and expected load values.

The major contributions of this paper are summarized as follows:

- A two-level optimal bidding strategy framework is proposed to estimate and quantify the change in total load under DR programs. The sum of the load of all consumers (without considering the impact on DR) is predicted using a data-driven forecasting model, and the change rate of each agent's load (considering the impact of DR) is estimated by D-ABM. Because both the forecasting model and D-ABM are based on time series data, the overall framework can be incorporated as a data-driven methodology.
- The proposed D-ABM defines all consumers as heterogeneous agents, meaning that each consumer becomes a unique agent using individual data. This approach is different from traditional ABM, which only considers the comfort associated with certain appliances (such as air conditioning or heating load) or groups consumer agents based on electricity consumption patterns and usage. Moreover, since the properties of each agent are extracted through statistical data analysis based on real data, D-ABM can provide improved realism and objectivity.
- As a strength of the bottom-up approach, D-ABM can assign different biases and preferences to each consumer agent, providing an opportunity for more realistic estimates of the impact of total load for DR implementation.
- By realistically estimating the impact of total load under DR through the proposed framework, it is possible to minimize any penalty costs due to deviations of the bidding strategy, ensuring maximum profits for the load aggregator.

D. PAPER ORGANIZATIONS

The remainder of this paper is organized as follows. In Section II, a two-level hybrid framework is explained that addresses uncertainties associated with the load aggregator's bidding strategy. Section III presents the problem formulation of the optimal bidding strategy and an overall flowchart of the proposed framework. Illustrative numerical simulation results are analyzed in detail in Section IV. Finally, the conclusions are summarized in Section V.

II. UNCERTAINTY MODELING

In this section, the uncertainties associated with a load aggregator's bidding strategy are addressed. At the aggregate level, following a two-level hybrid framework, the data-driven forecasting model predicts the total load of all consumers and electricity prices in the day-ahead wholesale market. Then, at the individual level, D-ABM is introduced to consider the degree of consumer participation in DR and the uncertainty of whether to participate. In addition, D-ABM emulates the usage patterns of the appliances for shiftable and controllable

loads where electricity consumption has a more right-skewed distribution especially.

A. LOAD AND MARKET PRICE FORECASTING

The load aggregator acts as an intermediary between end users and the network operator and needs to collect the necessary information (such as load and market price forecasting) to formulate an optimal bidding strategy. In this subsection, these uncertainties are handled through LSTM autoencoder-based forecasting and anomaly detection using a multivariate time series dataset.

1) MULTIVARIATE TIME SERIES DATA ANALYSIS

Time series forecasting is a technique for studying the behavior of temporal data (which is a collection of observations in chronological order) and predicting future values. Time series data can be divided into two broad categories: univariate and multivariate. Multivariate time series data has more than one time-dependent variable. Moreover, each variable is associated with its past value and, in some cases, is correlated with other variables in the dataset. Therefore, modeling all related variables together in these problems provides a better understanding compared to modeling each variable individually.

The general expression for multivariate time series forecasting is presented in (1). Here, the model input is a historical dataset containing the target y itself and other variables from the multivariate time series data. The goal of the model is to forecast the future temporal values from y_{t+1} at time $t+1$ to y_{t+p} at time $t+p$ based on a past time series dataset.

$$\underbrace{\begin{pmatrix} x_{t-l}^{(1)} & \cdots & x_{t-l}^{(n)} \\ \vdots & \ddots & \vdots \\ x_{t}^{(1)} & \cdots & x_{t}^{(n)} \end{pmatrix}}_{\text{multivariate time series data}} \overset{\text{model}}{\rightarrow} \begin{pmatrix} y_{t+1} \\ \vdots \\ y_{t+p} \end{pmatrix} \tag{1}$$

where l, n, and p represent the number of samples, the number of input variables, and the predicted size of multi-step forward forecasting, respectively.

Data preprocessing is initially performed, which is the foundation of effective data analysis. This is an indispensable step considering the intrinsic complexity of time series data and deficiencies in terms of data quality. Data preprocessing refers to a set of techniques for improving the quality of raw data, such as removing outliers and handling missing values. First, the data is passed to the data-cleaning step, where missing or defective data are treated with linear interpolation. Then, the cleaned data of each variable is scaled using the MinMaxScaler function, as represented by

$$x_{\text{scaled}}^{(i)} = \frac{x^{(i)} - x_{\min}^{(i)}}{x_{\max}^{(i)} - x_{\min}^{(i)}}, \qquad i = 1, \ \ldots \ , n \tag{2}$$

where $x_{\max}^{(i)}$ and $x_{\min}^{(i)}$ are the maximum and minimum values of the data of each variable $x^{(i)}$, respectively.

Although the high dimensionality and spatiotemporal dependence of multivariate time series data render them useful for predicting future values, they contain noisy data. One of the feature extraction methods is PCA [22], which is a dimensionality-reducing multivariate statistical method that can transform original multiple correlated variables into several linearly uncorrelated principal components. The information contained in the principal components does not overlap and is not interrelated. Moreover, selecting a few principal components with high contributions can reflect most of the information in the original variable. Thus, PCA is applied to convert a high-dimensional data set into a low-dimensional data set. By using PCA, noise and redundant data can be reduced while preserving as much of the important information from the original data set as possible.

2) LSTM AUTOENCODER

Time series data usually refers to a sequence of values measured continuously or discretely over time. In time series forecasting tasks, the complexity of sequence dependencies among the input variables must be considered. Recurrent neural networks (RNNs) are a powerful type of NN for addressing these sequence dependencies. Moreover, an RNN has a feedback loop in the hidden layer of the NN, through which it can be influenced by the output of the previous time step, providing some level of memory within the network itself. However, in traditional RNNs, as the distance between the relevant information and the point where it is used increases, the gradient gradually decreases during backpropagation, resulting in a significant decrease in learning ability. LSTM has been proposed to overcome the vanishing or exploding gradient problems of the RNN training process [23]. LSTM networks are a modified form of RNNs with state memory and multi-layered cell structures to learn long-term dependence information.

In LSTM architecture, the processing state is recorded in the cell and there are gate mechanisms (forget, input, output, and update gates) to control the information in the cell. The forget gate decides which information to discard, while the input gate determines which new information should be recorded into the cell state. The update gate refers to the process of updating from a past cell state c_{t-1} to a cell state c_t, while the output gate determines how much information in the current cell is assigned to the next cell. The mathematical representation of the LSTM model is as follows:

$$f_t = \sigma(W_{xf}^T \cdot x_t + W_{hi}^T \cdot h_{t-1} + b_i) \tag{3}$$
$$i_t = \sigma(W_{xi}^T \cdot x_t + W_{hi}^T \cdot h_{t-1} + b_f) \tag{4}$$
$$o_t = \sigma(W_{xo}^T \cdot x_t + W_{ho}^T \cdot h_{t-1} + b_o) \tag{5}$$
$$g_t = \tanh(W_{xg}^T \cdot x_t + W_{hg}^T \cdot h_{t-1} + b_g) \tag{6}$$
$$c_t = f_t \otimes c_{t-1} + i_t \otimes g_t \tag{7}$$
$$y_t, h_t = o_t \otimes \tanh(c_t) \tag{8}$$

where f_t, i_t, o_t, and g_t are the output values of the forget, input, output, and update gates, respectively. The inputs of each gate include the input data x_t at a present time step t and the LSTM output value h_{t-1} at a former time step t-1. Terms $W_{xf,xi,xo,xg}$ and $W_{hf,hi,ho,hg}$ are the weight matrices

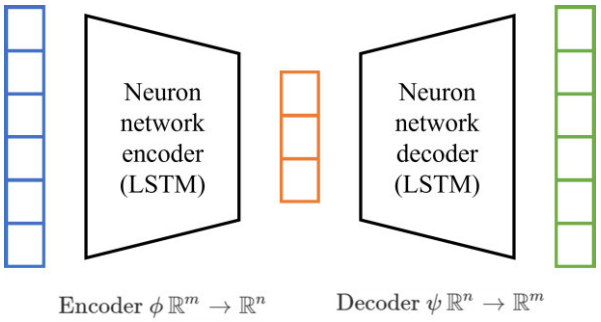

FIGURE 1. Schematic structure of LSTM autoencoder network.

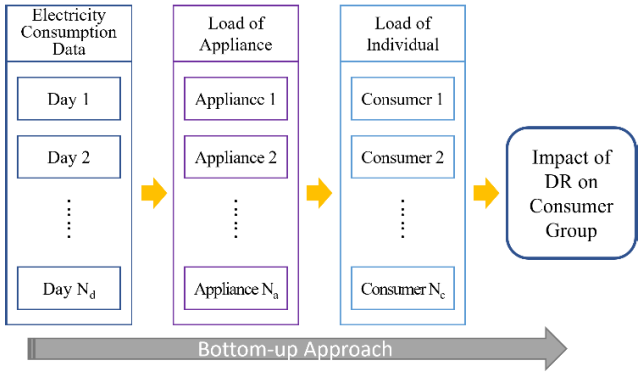

FIGURE 2. D-ABM in a bottom-up modeling approach.

of x_t and h_{t-1}, respectively, while $b_{f,i,o,g}$ are bias vectors and c_t and c_{t-1} indicate the cell states at times t and t-1, respectively. Term σ is the sigmoid activation function.

LSTM can be applied to both time series forecasting and anomaly detection due to its nature of learning patterns in data over long sequences. An autoencoder is a type of deep NN that performs two main tasks. First, it compresses a high-dimensional input into a lower-dimensional latent vector representation. Then, it uses this latent vector to reconstruct the original input. The autoencoder is composed of two major components: an encoder (which projects the input into the latent vector) and a decoder (which maps the latent vector back to the original space to reconstruct the input). The basic version of an autoencoder consists of three fully connected layers: input, hidden, and output. However, conventional autoencoders have limitations in terms of capturing temporal dependencies effectively. To address this issue, we adopted an LSTM autoencoder, which uses gate mechanisms to extract temporal dependencies more efficiently. Through this measure, the forecasting accuracy of load and market prices is increased. Among the available autoencoders, the LSTM autoencoder refers to configuring both the encoder and the decoder as an LSTM network, as displayed in Fig. 1 [24]. In this symmetrical structure, the encoder captures the most representative features of the input data using a small feature space, while the decoder reconstructs the input data based on the encoded features of the small feature space. Reconstruction errors are minimized through the learning process of the autoencoder. The autoencoder uses small feature spaces to maintain important information while reducing the data dimension; hence, it is likely to fail when reconstructing an anomaly. These deviations between the original input data and the reconstructed data can be an indicator of anomalies [2]. In other words, the ability of a trained autoencoder to reconstruct given input data provides insights into the normality of the input sequences. This means that the magnitude of the autoencoder's reconstruction error indicates that there is an anomalous vector within the data.

In this study, an LSTM Autoencoder was adopted as a data-driven forecasting model for anomaly classification, and the anomaly detection result was then used as a reference for load aggregator decision-making. Among the various methods for classifying anomalies, using predictive modeling defines an anomaly score based on the difference between predicted and newly observed values [25]. The mean absolute error (MAE) of (9) was adopted for the reconstruction loss calculation.

$$\mathrm{MAE} = \frac{1}{N} \sum_{t=1}^{N} \left| y_t - \hat{y}_t \right| \tag{9}$$

where N is the subsequence length and y_t, $\hat{y}_t$ are the actual and predicted values, respectively. Because there are no anomaly labels, the thresholds for anomaly detection can be very difficult to define. By sorting MAE in descending order, a threshold value for classifying anomalies can be selected.

B. PRICE-RESPONSIVE LOAD UNCERTAINTY

In this subsection, uncertainties in the price-responsive load for DR participation are addressed using D-ABM. In the context of ABM, D-ABM estimates emergent phenomena for changes in power consumption patterns caused by consumer agents with DR-related properties, and their interactions are defined by basic rules.

1) ABM

ABM is an approach for defining and capturing the dynamics of complex systems. These systems typically contain heterogeneous subsystems or autonomous entities and are often characterized by non-linear relationships and multiple interactions between them [26]. ABM is a simulation method that represents the phenomenon in which autonomous and adaptive agents interact within a given environment, rendering it useful for modeling the previously mentioned properties of complex systems [27]. In ABM, the environment is populated by autonomous beings that interact through prescribed basic rules. Furthermore, ABM is a bottom-up approach that allows observing the resulting emergent behavior of the system through the basic rules of individual behavior and collective interactions. These aspects allow it to predict or envision phenomena of interest by focusing on the uniqueness of individuals and the interactions between them. ABM also models a variety of heterogeneous behaviors at the individual

level, and these individual behaviors result in expressing the emergent phenomenon at the global level. While an individual agent's behavior is based on limited information at the micro level, the resultant emerging behavior of the system can be derived and analyzed at the macro level.

Unlike conventional mathematical models that consider a homogenous population, agent-based approaches can be modeled by reflecting individuals with distinct characteristics. To quantify the various effects on the aggregated load under a certain scheme of DR through D-ABM, the load of each consumer agent is decomposed to the appliance level, as displayed in Fig. 2. These loads of each agent are classified into five types according to the degree of flexibility: a) shiftable loads (e.g., dishwashers and washing machines); b) controllable loads (e.g., air-conditioners and heating systems); c) storable loads (e.g., EVs); d) on-demand loads (e.g., lighting and televisions); and e) base loads (e.g., refrigerators). Here, shiftable loads are appliances that can transfer electricity consumption to other times without affecting normal service, whereas controllable loads are appliances that can reduce consumption without affecting the occupants' comfort or quality of life. On-demand loads are appliances that meet the needs of occupants' living and entertainment [28]. Accordingly, shiftable loads have the greatest potential for participation in DR, followed by controllable and on-demand loads. Base loads have no potential for participation in DR.

In our study, only three groups of appliances were considered for estimating the individual potential of each consumer to participate in DR: shiftable loads, controllable loads, and other loads. Each consumer agent has a unique number of appliances and different usage patterns for individual appliances. Therefore, these facts become the properties of each agent derived through statistical data analysis as the initial condition of D-ABM.

In the context of ABM, the behavior and interactions of complex systems composed of heterogeneous agents can be defined by simple rules and assumptions. Herein, changes in the electricity consumption patterns of each agent due to DR is emulated closely to the real phenomena through basic rules. Moreover, uncertainties about agents' behaviors are addressed from several assumptions about behavioral economics that explain bounded rationality. From these simple rules and assumptions, our model focuses on modeling the uncertainties of heterogeneous consumer agents' decision-making and the consequent variety of collective phenomena. Details of D-ABM will be discussed in the following subsections.

2) D-ABM

The starting point of ABM is to identify a set of facts and empirical regularities, such as observed distributions and static or dynamic correlations [29]. The input of ABM can be characterized into two broad categories: initial conditions and parameters. Initial conditions in complex systems are not easily identified and are not well-known to modelers. To extract the characteristics of these agents more realistically and objectively from data, this study proposes D-ABM based on a statistical data analysis. The heterogeneous properties of each agent in D-ABM are defined from a specific statistical distribution that represents empirical regularities according to the data analysis. Electricity consumption patterns of individual household consumers are usually irregular, exhibit strong randomness, and depend on various factors (including the features of dwellings, the diversity of home appliances, and the behavior of occupants). Seasonal and diurnal variations also have an effect. ABM provides an opportunity to model these heterogeneous usage patterns that reflect multiple factors. In D-ABM, each consumer agent has the following two properties as random values derived from the probability distribution function of its actual electricity consumption data: a) individual total load consumption and b) shiftable and controllable load consumption.

Individual total load consumption is a non-negative integer that has a right-skewed distribution at each time resolution in the dataset. Low and moderate electricity consumption is more common, while high electricity consumption is relatively rare. Therefore, the probability distribution that fits the dataset will be asymmetrical. Herein, a box-cox transformation was applied to generate random values that would be as close as possible to the distribution of the actual data. Box-cox transformation is a power transformation method that integrates, extends, and improves traditional transformation methods (such as log, square root, and inverse), enabling researchers to easily find optimal normalization transformations for each variable [30]. Moreover, it can meet statistical assumptions (i.e., normality, and homogeneity of variance) by improving the normality of the distribution over the dataset and stabilizing the variance.

$$w_t = \begin{cases} \log(y_t), & \lambda = 0; \\ (y_t^{\lambda} - 1)/\lambda, & \lambda \neq 0. \end{cases} \tag{10}$$

Depending on parameter λ, (10) indicates that a variable can be effectively transformed to move to normality, regardless of whether it is negatively or positively skewed. A random value is generated from the statistical distribution processed through the box-cox transformation of each time resolution data. Then, this value is inverted and provided as agent properties for expected individual total load consumption values.

Appliance-level electricity consumption has a more right-skewed distribution, especially for shiftable and controllable loads. Moreover, the frequency of use is relatively intermittent, and consumption is generally low (close to zero) except when in use. Gamma distribution was adopted to generate random values that would represent the distribution of data for these appliances at each time resolution, which is defined as follows:

$$f(x;\ a,\ b) = \frac{x^{a-1}}{\Gamma(a)b^a} \exp(-\frac{x}{b}),\quad a,\ b\ >\ 0 \tag{11}$$

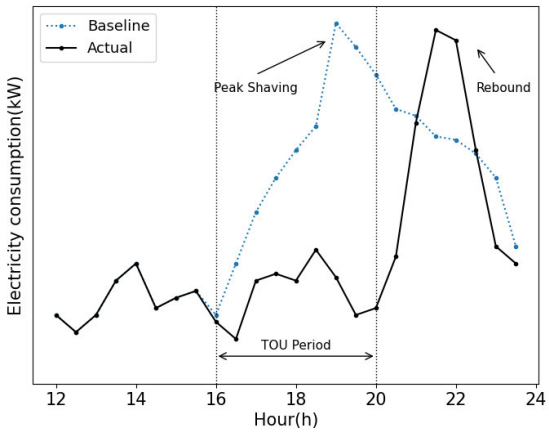

FIGURE 3. Daily electricity consumption profile affected by DR.

Here, Γ is the gamma function and x, a, b are a random variable, the shape parameter, and the scale parameter, respectively. The expected electricity consumption values for each appliance at each time resolution are assigned as random values based on the gamma distribution of the data for that time resolution. These statistical analyses can capture when and to what extent a particular appliance is likely to be used.

The behavior and interactions of consumer agents can be defined by basic rules and assumptions in the context of ABM. In our study, the basic rule is defined based on the collective phenomenon that appears as the electricity tariff system applied to each consumer agent changes. In particular, we explore the changes in consumer's electricity consumption pattern under the TOU tariffs, which guarantees the consumer's degree of freedom among various DR programs and can provide consumers with certainty about price information at different times [31].

With TOU tariffs, days are divided into several periods (usually less than five), and different fixed rates are used for peak and off-peak periods. This encourages rational consumers to permanently change their energy consumption based on differential electricity rates. Fig. 3 illustrates typical changes in consumption patterns under the TOU program. This is termed "Peak Shaving and Rebound" as a collective phenomenon, which is a result of changing consumer behavior under TOU [32]. As a basic rule for changes in consumption patterns of each appliance, price-responsive shiftable loads are likely to shift entirely to an adjacent time period when rates are lower. Moreover, the consumption of price-responsive controllable loads is likely to simply reduce to an extent that does not impair consumer comfort. Basic rules emulating these phenomena can be formulated as follows:

$$P_{t,i}^{shift} = \Big(\sum_{t=T_{DR}} P_{t,i}^{shift}\Big) \cdot \alpha_1^{shift} \ \forall t \in \{t_{DR}^{start} - \Delta t_1, \ldots, t_{DR}^{start}\} \tag{12}$$

$$P_{t,i}^{shift} = \Big(\sum_{t=T_{DR}} P_{t,i}^{shift}\Big) \cdot \alpha_2^{shift} \ \forall t \in \{t_{DR}^{end}, \ldots, t_{DR}^{end} + \Delta t_2\} \tag{13}$$

$$P_{t,i}^{control} = Req(P_{t,i}^{control}) \cdot \alpha^{control} \ \forall t \in \{t_{DR}^{start}, \ldots, t_{DR}^{end}\} \tag{14}$$

$$s.t \alpha_1^{shift} \cdot \Delta t_1 + \alpha_2^{shift} \cdot \Delta t_2 = 1 \tag{15}$$

where $T_{DR} = \{t | t_{DR}^{start}, \ \ldots \ , \ t_{DR}^{end}\}$ is a set of timeslots during the DR duration period and the time resolution $\Delta t = 15$ min. Terms $P_{t,i}^{shift}$ and $P_{t,i}^{control}$ are the electricity consumption of i^{th} the consumer's shiftable load and controllable load at time t, respectively. Term $Req(P_{t,i}^{control})$ is the electricity consumption of the controllable load originally required, while α_1^{shift}, α_2^{shift}, and $\alpha^{control}$ are the coefficients of change in each appliance's usage due to DR participation. These coefficients determine the degree of load change due to DR in (12), (13), and (14), while (15) means that the electricity consumption of the shiftable load remains constant before and after DR.

The purpose of D-ABM interactions is to estimate changes in collective electricity consumption patterns from the independent decision-making results of each agent. In the real world, each household has no related information on the electricity consumption and behavior of other households, and their impact on each other is insignificant. Furthermore, the behavior of each agent is not homogeneous. Therefore, various changes in electricity consumption patterns are estimated herein by taking advantage of ABM, which is a bottom-up approach. The bottom-up approach can quantify the results of various interactions considering the irrationality of consumer decision-making by assigning "bias and preference" to each agent. This is one of the theories of behavioral economics.

Behavioral economics combines elements of psychology with classical economics to incorporate fundamental, persistent, and consistent biases into individual decision-making [33]. Because D-ABM simply uses it to assume a situation of bounded rationality for individual decision-making, a more detailed explanation of behavioral economics is considered beyond the scope of this paper. Ultimately, the goal of this study is to model more realistic DR participation rates by imposing assumptions related to bounded rationality on specific agents. Several assumptions about behavioral economics (in terms of interactions) are described in more detail in the simulation process of Section IV.

III. OPTIMAL BIDDING STRATEGY

In this work, the main purpose of the load aggregator's bidding strategy is to maximize their profit. This is achieved by determining the optimal bid quantity for each hour in the day-ahead markets and minimizing penalty costs resulting from load deviations, as depicted in Fig. 4. Specifically, in the aggregated level, the total load and market prices are forecasted based on the LSTM autoencoder. Simultaneously, at the individual level, the D-ABM addresses the uncertainty of individual consumers' price responsiveness when participating in DR. The proposed D-ABM estimates the rate of change of the total load resulting from demand response activities. Finally, considering the uncertainties addressed

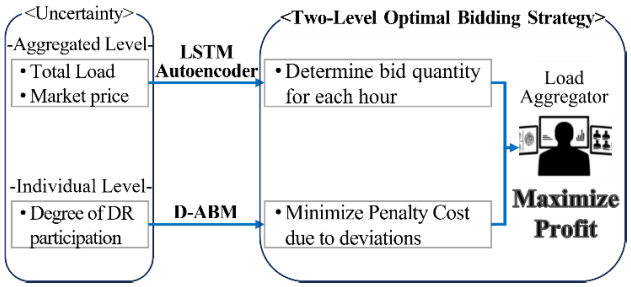

FIGURE 4. Framework of optimal bidding strategy for load aggregator.

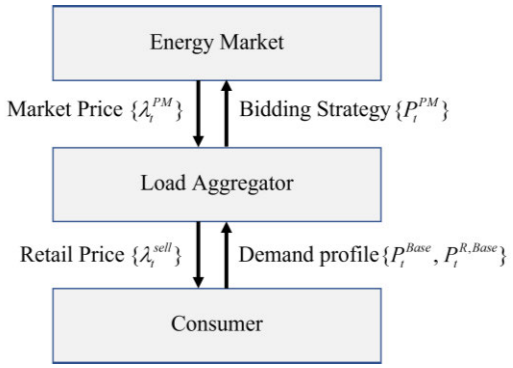

FIGURE 5. Interactions with load aggregator and related business entities.

at each level, the proposed framework can determine the load aggregator's bidding strategy in day-ahead markets. This ensures maximum profit by reducing any deviations between actual and expected load values. Specific details of the proposed two-level bidding framework are illustrated in the following subsections.

A. PROBLEM FORMULATION

As mentioned previously, load aggregators act as intermediaries that interact with end users and network operators. However, unlike the unidirectional exchange of information in traditional power systems, the addition of load aggregators (including DR) means that the entire market requires more interactions, adding complexity. These bi-directional interactions with load aggregators and related business entities are illustrated in Fig. 5. In the relationships between consumers and load aggregators, downward interactions refer to retail price information, while upward interactions refer to the demand profile information. In the relationship between the wholesale market and load aggregators, downward interactions refer to market price information, while upward interactions refer to bidding strategies.

Based on Fig. 5, the aim of load aggregators' bidding strategies is to maximize profits by optimally determining the hourly bid quantity in day-ahead markets and minimizing penalty costs due to deviations. This is formulated as follows:

$$MaxR_{Agg} = \sum_{t=1}^{N^t} \left\{ (R_t^{sell}) - (C_t^{PM} + C_t^{P,Base}) \right\} \tag{16}$$

$$R_t^{sell} = P_t^{sell} \times \lambda_t^{sell} \ \forall t \tag{17}$$

$$C_t^{PM} = P_t^{PM} \times \lambda_t^{PM} \ \forall t \tag{18}$$

$$C_t^{P,Base} = \sum_{t=1}^{N^t} \lambda_t^{RR} \times \max[0, (P_t^{Base} - P_t^{R,Base})] + \sum_{t=1}^{N^t} \pi_1 \times \max[0, (P_t^{R,Base} - P_t^{Base})] \ \forall t \tag{19}$$

$$P_t^{PM} = P_t^{Base} \ \forall t \tag{20}$$

The aim of the objective function provided by (16) is to maximize the profits for the load aggregators. (17) for R_t^{sell} represents the revenue from selling electricity to consumers, where P_t^{sell} and λ_t^{sell} are the amounts of electricity sold to consumers and the retail prices, respectively. (18) for C_t^{PM} represents the cost of purchasing electricity from the wholesale power market, where P_t^{PM} and λ_t^{PM} are the amount of electricity purchased from the market and the price of day-ahead power markets, respectively. (19) for $C_t^{P,Base}$ represents the penalty cost of load due to forecasting deviations, where P_t^{Base} and $P_t^{R,Base}$ are the predicted and actual values of the baseline load and λ_t^{RR} and π_1 are the price of reserve requirement and the penalty coefficients of the load, respectively. The power balance constraint in (20) means that the supply P_t^{PM} and demand P_t^{Base} of the load aggregator must be equal.

In this study, the load aggregators act as price-takers in the wholesale market, given their relatively small capacities [34]. Therefore, by utilizing the uncertainties (related to market price, total electricity consumption, and price-responsive load) handled through the proposed framework, it is possible to reduce penalty costs due to bidding strategy deviation and to ensure maximum profits.

B. OVERALL PROCEDURE

The overall procedure of the proposed data-driven two-level optimal bidding strategy framework is displayed in Fig. 6 and can be performed according to the following steps:

Step 1: Collect multivariate time series data for data-driven forecasting modeling and the D-ABM.

Step 2: Perform data preprocessing in data-driven forecasting models, which comprises a series of processes, including data cleansing, normalization, and feature extraction.

Step 3: Construct a forecasting model based on the LSTM autoencoder, which features a reconstruction process. It can also be utilized for anomaly detection.

Step 4: Forecast the aggregate load of a consumer group and market price. The predicted values are then used as input data to the load aggregator's bidding strategy.

Step 5: As a starting point for the D-ABM stage, assign each agent's two properties via statistical analysis of their unique personal data at each time resolution: a) individual total load consumption and b) shiftable and controllable load consumption.

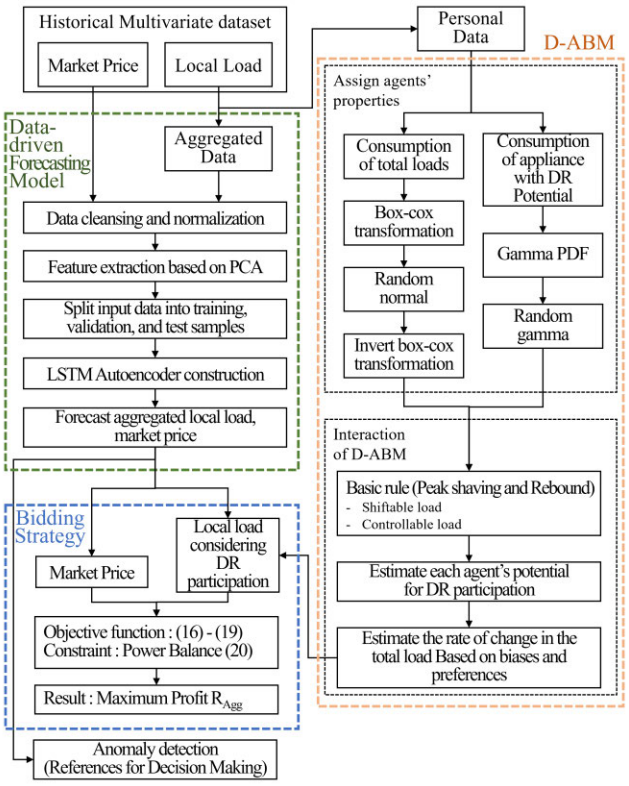

FIGURE 6. Flowchart of the proposed bidding strategy framework.

Step 6: Generate random values that emulate the agents' actual electricity consumption patterns. The value of a) is obtained from a normal distribution with a box-cox transformation, while the value of b) is obtained from a gamma distribution.

Step 7: Calculate the potential for DR participation of each agent with heterogeneous properties by applying basic rules that emulate phenomena based on an institutional framework.

Step 8: Estimate the rate of change in the total load from interactions by assuming different situations regarding biases and preferences.

Step 9: Optimize the load aggregator's bidding strategy based on the expected deviation from a comparison between each scenario in Step 8.

IV. NUMERICAL SIMULATION

The proposed data-driven two-level optimal bidding strategy was numerically simulated using actual data. The load aggregator was assumed to participate in the day-ahead power market on behalf of residential loads. The load data was a 15-min time-resolution time-series data from the Pecan Street dataport [35], from which the data of 11 households without solar power were selected from a total of 25 households in New York from 1 May 2019 to 31 Oct. 2019. This also included electricity usage according to each appliance, and each agent had different appliances based on their personal ownership status. The price data was time-series data with

TABLE 1. Parameter settings.

Parameter	Value	Parameter	value
λ_t^{RR} , π_1 (\$/kWh)	0.025	α_1^{shift}	0.06
α_2^{shift}	0.095	$\alpha^{control}$	0.9

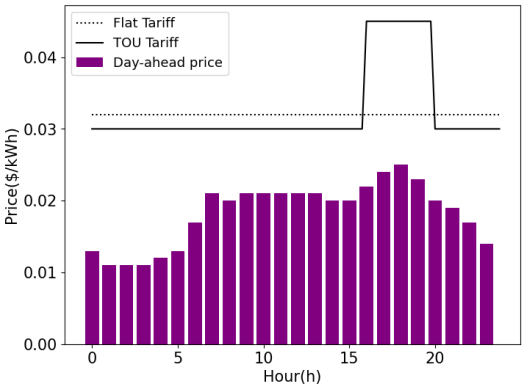

FIGURE 7. Day-ahead market and retail prices.

1-h intervals for the NYISO's day-ahead wholesale market from 1 Nov. 2017 to 31 Oct. 2019 [36]. Additionally, other historical data (such as the weather, day of the week, and natural gas prices) were included as multivariate variables for predictions in the data-driven forecasting model. Fig. 7 displays the retail prices (λ_t^{sell}) and day-ahead market prices (λ_t^{PM}) that were adopted. Here, flat and TOU tariffs were applied to the retail price. Table 1 depicts several important parameter settings used for the numerical simulations [37].

The evaluation metric of the data-driven forecasting model is as follows: RMSE (Root Mean Square Error) and R^2(Coefficient of Determination).

$$\mathrm{RMSE} = \sqrt{\frac{1}{N}\sum_{i=1}^{N}(y_i^{actual} - y_i^{predict})^2} \tag{21}$$

$$\mathrm{R}^2 = 1 - \sum_i (y_i^{predict} - y_i^{actual})^2 / \sum_i (y_i^{average} - y_i^{actual})^2 \tag{22}$$

where y_i^{actual} is an actual value of testing samples; $y_i^{predict}$ is the forecasting result of y_i^{actual}; and N is the total number of testing samples. The R^2measure indicates the extent to which the variance of the forecasted value validates the variance of the actual value. The simulations for the data-driven forecasting model and D-ABM were implemented based on Python's TensorFlow and libraries and were performed on a platform with a 3.4GHz Intel(R) Core (TM) i7 and 16GB of RAM.

A. DATA-DRIVEN FORECASTING RESULTS

The collected multivariate time series dataset for the prediction of aggregated load and market price contained 17664 samples/21 features and 17520 samples/17 features, respectively. For more accurate predictions and improved

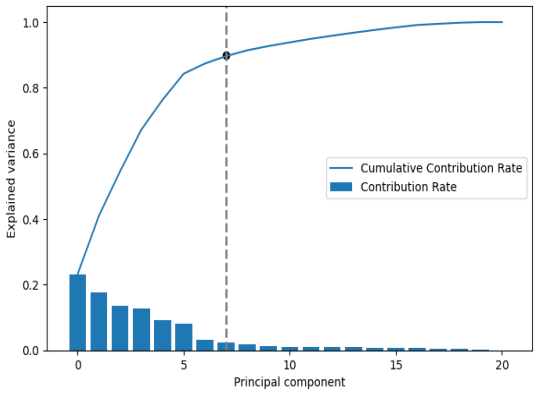

(a) Load

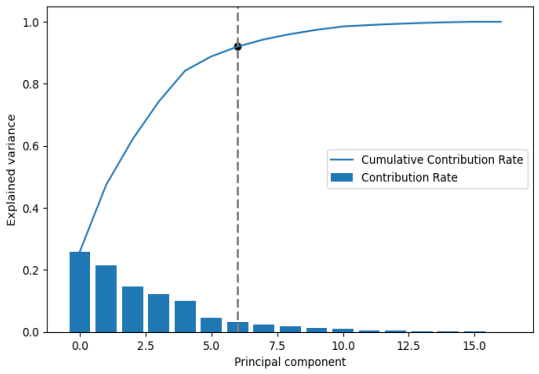

(b) Market price

FIGURE 8. Dimension reduction by PCA.

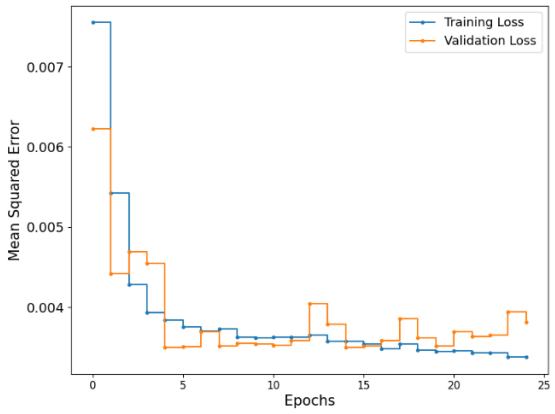

(a) Load

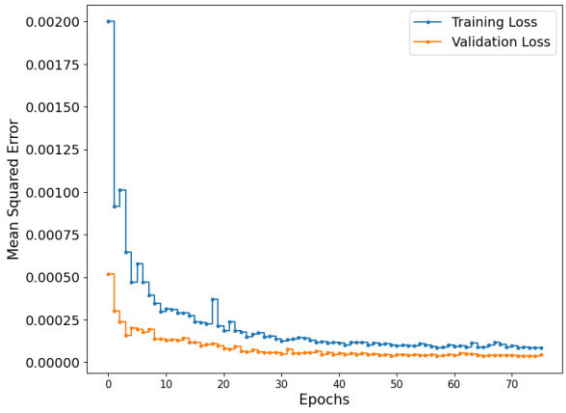

(b) Market price

FIGURE 9. Learning curve results.

computational efficiency, the dataset was dimensionally reduced using the PCA algorithm, as presented in Fig. 8. According to the contribution rate and the cumulative contribution rate of each component, seven and six principal components representing a cumulative contribution rate of 90% or more were selected, respectively.

For training and forecasting the model, 70%, 15%, and 15% of the dataset were assigned to training, validation, and test samples, respectively. The LSTM autoencoder forecasting model employed in this study contained four hidden LSTM layers, each with 100, 50, 50, and 100 neurons. The learning rate, optimizer, activation, and loss functions were 0.001, Adam, Relu, and MeanSquaredError, respectively. These model hyperparameters were all designed using a trial-and-error method. Early stopping was also adopted to reduce training costs and prevent overfitting. Fig. 9 displays the loss function for each training and validation dataset in the training process. It should be noted that the hyperparameters are optimized so that the difference between the loss functions is negligible without overfitting and convergence problems. After training the model, the next step involved using it to make predictions.

To demonstrate the superiority of the LSTM autoencoder, Table 2 displays a comparison between the prognostic performances on the test dataset of the LSTM autoencoder and three well-established prediction models (LSTM, CNN, and CNN-LSTM). Here, the RMSE values of the LSTM autoencoder for aggregated load and market price were 1.577 and 1.308, respectively, compared to 1.618 and 1.405, respectively, for the CNN-LSTM model. The R^2 values of the market price and aggregated load for the LSTM autoencoder were 0.9546 and 0.7603, respectively. Typically, individual loads fluctuate widely and are highly random, while market prices are relatively stable. Accordingly, the forecasting results for market prices tend to be more accurate. In particular, since the number of aggregated loads in this paper was small, the variability of the individual loads remained in the aggregated loads, as evidenced by the low R^2 value.

TABLE 2. Forecasting error criteria.

Forecasting model	Aggregated Load		Market Price	
	RMSE	R^2	RMSE	R^2
LSTM	1.641	0.7404	1.664	0.9266
CNN	1.656	0.7359	1.619	0.9305
CNN-LSTM	1.618	0.7479	1.405	0.9477
LSTM Autoencoder	1.577	0.7603	1.308	0.9546

Fig. 10 illustrates the forecasting and anomaly detection results for the test dataset using the LSTM autoencoder. As displayed in Fig. 10(a), the model usually captured the trend of change for the aggregated load, although it exhibited

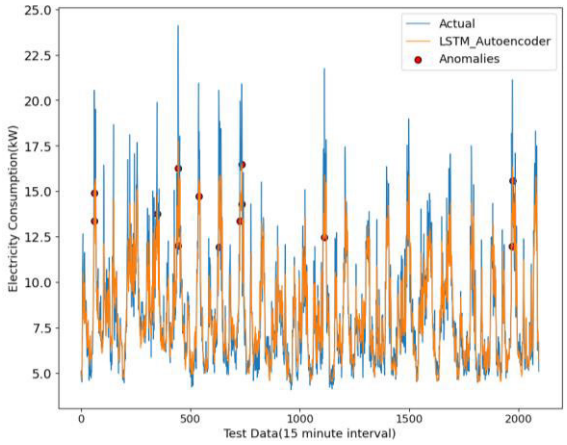

(a) Load

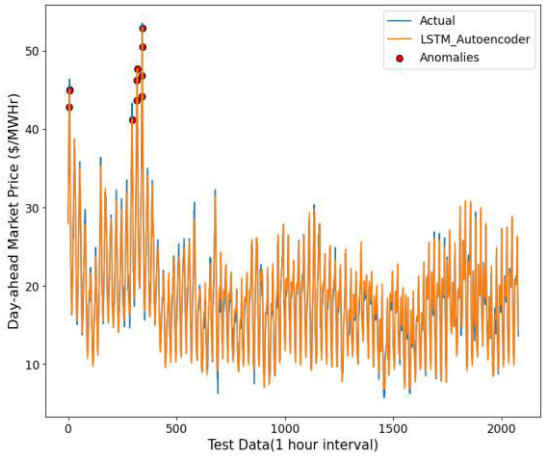

(b) Market price

FIGURE 10. Forecasting results and anomaly detection of LSTM autoencoder model.

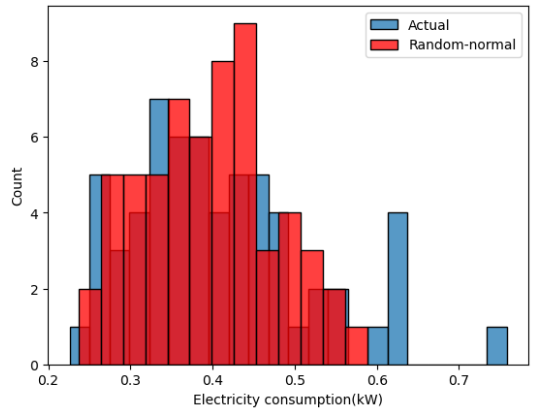

(a) Histogram at 00:15 time zone

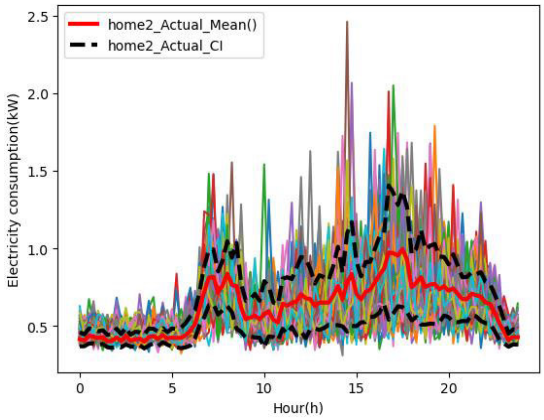

(b) 24-h electricity consumption

FIGURE 11. Comparison of actual and D-ABM values for total electricity consumption.

gaps caused by values for unexpected variations. To detect unexpected variations, the threshold applied to anomaly detection was 0.4513, which was the top 5th value of MAE in the training dataset. Here, the number of anomalies was 13, which occurred evenly over the entire time horizon. The forecasting values for the market price in Fig. 10(b) exhibited small differences from the actual values, and the LSTM autoencoder displayed more accurate forecasting performance. In this case, the threshold applied to anomaly detection was 0.0846, which was the top 5th value of MAE in the training dataset, in which there were 11 anomalies. These anomalies were concentrated on a specific day, and no anomalies were found during the rest of the period. In addition, when 0.138 was set as the threshold (the highest value of the MAE of the training dataset), no anomalies were found in the test dataset.

B. D-ABM RESULTS

The purpose of D-ABM is to derive the rate of change in the total load more realistically. In this context, the properties of each consumer agent were divided into two categories: a) consumption of total loads and b) consumption of shiftable and controllable loads with DR potential. Since the usage patterns of individual home appliances often follow periodic and seasonal characteristics, only data from adjacent periods (60 days in this simulation) with similar weather data were used as the input values for D-ABM.

Fig. 11 depicts a comparison between the actual data for the total electricity consumption of home2 and the value modeled via D-ABM. Here, the entire data was selected from two months (Sep. and Oct.) of data that exhibited similar electricity consumption patterns due to the influences of seasonality and the weather. The results in Fig. 11(a) demonstrate that each dataset exhibited a similar distribution and had slight differences that could be regarded as randomness in the real world. Fig. 11(b) presents the 24-h electricity consumption of home2 at 96-h resolution (15)-min intervals). Here, the bold line is the average of the actual data over the period and the dashed line represents the 99% confidence interval. The total number of iterations is 100. Most of the random values were included in the confidence interval and only some were outside the confidence interval. Accordingly, this result realistically emulated the intermittence and randomness of actual electricity consumption.

TABLE 3. Appliance list and consumption patterns of consumer agents.

Home	Ownership of Home Appliances	Electricity Consumption at TOU (kWh)
Home1	{'dishwasher1', 'drye1', 'furnace1', 'kitchenapp1', 'kitchenapp2', 'livingroom1'}	4.17
Home2	{'clotheswasher1', 'drye1', 'furnace1', 'kitchen1', 'kitchenapp1', 'kitchenapp2', 'range1'}	5.47
Home3	{'clotheswasher1', 'drye1', 'kitchenapp1','livingroom1', 'range1'}	2.76
Home4	{'kitchen1', 'livingroom1', 'microwave1', 'oven1'}	4.84
Home5	{'clotheswasher1', 'dishwasher1', 'drye1', 'furnace1', 'kitchenapp1'}	4.63
Home6	{'clotheswasher1', 'drye1', 'furnace1', 'heater1', 'heater2', 'livingroom1', 'range1'}	10.35
Home7	{'clotheswasher1', 'dishwasher1', 'drye1', 'kitchenapp1', 'kitchenapp2'}	14.78
Home8	{'clotheswasher1', 'dishwasher1', 'drye1', 'kitchenapp1', 'kitchenapp2'}	6.42
Home9	{'clotheswasher1', 'dishwasher1', 'drye1', 'range1'}	8.39
Home10	{'clotheswasher1', 'dishwasher1', 'drye1', 'furnace1',}	7.12
Home11	{'dishwasher1', 'furnace1', 'kitchenapp1','kitchenapp2'}	3.75

TABLE 4. Potential for DR participation of consumer agents.

	Potential for DR participation (%)																											
	15:00	15:15	15:30	15:45	16:00	16:15	16:30	16:45	17:00	17:15	17:30	17:45	18:00	18:15	18:30	18:45	19:00	19:15	19:30	19:45	20:00	20:15	20:30	20:45	21:00	21:15	21:30	21:45
home1	26.96	27.28	30.66	29.8	-25.45	-24.79	-23.54	-19.98	-22.64	-24.59	-21.5	-24.31	-17.31	-18.85	-16.12	-21.17	-17.11	-19.15	-20.85	-26.82	19	17.99	18	17.38	17.19	19.58	17.55	18.11
home2	25.25	24.31	24.59	23.68	-20.39	-15.29	-18.28	-18.35	-22.18	-21.29	-19.49	-17.37	-18.52	-19.7	-15.41	-16.19	-15.44	-16.21	-15.28	-18.29	23.06	24.9	24.2	20.86	22.18	21.59	23.28	23.36
home3	12.14	13.09	11.75	12.1	-3.58	-4.48	-3.67	-4.94	-7.99	-7.9	-12.16	-15.88	-13	-14.47	-12.33	-14.39	-9.92	-11.77	-10.57	-7.8	5.62	6.79	6.1	7.48	7.57	8.17	8.38	10.04
home4	18.83	18.83	18.96	18.29	-7.6	-5.17	-11.78	-13.2	-13.99	-15.54	-13.01	-11.98	-11.12	-10.55	-11.55	-11.43	-10.45	-9.51	-10.24	-7.57	14.17	14.34	14.92	15.4	16.38	16.95	17.3	17.37
home5	8.35	8.56	7.61	7.41	-4.61	-5.21	-5.1	-6.49	-4.82	-6.75	-4.78	-5.55	-4.23	-5.58	-7.19	-6.74	-7.64	-5.8	-5.31	-4.1	4.91	4.71	4.5	4.54	4.48	4.75	4.63	4.54
home6	0.17	0.17	0.17	0.17	-2.98	-2.98	-3.08	-2.31	-3.13	-4.32	-3.47	-4.21	-4.72	-4.26	-3.61	-3.98	-3.14	-3.1	-2.45	-2.44	0.15	0.15	0.16	0.15	0.17	0.17	0.16	0.17
home7	8.24	7.9	7.96	7.97	-6.23	-4.37	-3.96	-4.48	-5.21	-4.98	-4.15	-3.95	-4.08	-3.46	-6.53	-5.62	-4.46	-5.97	-7.72	-5.57	5.73	6.12	6.13	6.43	6.56	7.27	7.56	8.1
home8	35.46	28.66	31.66	28.89	-28.18	-30.73	-27.59	-28.59	-22.37	-23.53	-19.69	-24.77	-18.53	-15.93	-17.83	-19.63	-13.15	-18.67	-23.36	-23.54	20.72	16.56	14.23	18.15	18.35	19.01	26.56	26.13
home9	2.58	2.47	2.58	2.74	-1.17	-3.27	-1.85	-2.04	-1.79	-2.22	-2.3	-2.73	-2.91	-2.34	-2.48	-1.23	-1.82	-2.26	-1.72	-1.78	0.88	0.9	0.87	0.92	0.96	0.96	0.95	0.96
home10	5.7	5.69	5.53	5.41	-1.69	-2.48	-0.89	-2.03	-5.11	-4.27	-3.67	-2.1	-2.52	-2.39	-3.81	-3.52	-6.67	-6.21	-6.56	-6.07	3.32	3.65	3.94	3.71	3.97	4.06	4.17	4.95
home11	11.09	11.09	10.69	10.43	-7.78	-7.04	-6.57	-7.3	-8.18	-7.47	-6.41	-7.87	-9.16	-6.67	-4.92	-5.72	-5.5	-4.76	-5.14	-6.25	8.83	8.47	8.8	8.01	8.64	9.21	9.49	9.67

TABLE 5. Rate of change in the total load according to scenario.

	The Rate of Change in The Total Load (%)																											
	15:00	15:15	15:30	15:45	16:00	16:15	16:30	16:45	17:00	17:15	17:30	17:45	18:00	18:15	18:30	18:45	19:00	19:15	19:30	19:45	20:00	20:15	20:30	20:45	21:00	21:15	21:30	21:45
Scenario 1	7.2	7.1	7.1	6.8	-5.0	-3.8	-4.8	-4.9	-5.5	-5.1	-4.8	-5.1	-4.6	-4.9	-4.7	-4.4	-3.9	-4.3	-4.2	-4.0	4.5	4.6	4.7	4.9	5.1	5.6	6.2	7.0
Scenario 2	15.4	14.3	14.9	14.2	-12.2	-9.9	-12.9	-11.8	-11.2	-11.0	-9.8	-9.6	-8.5	-8.8	-8.3	-8.0	-6.7	-8.2	-7.0	-8.6	10.0	10.1	9.2	10.0	10.9	11.0	12.3	14.9
Scenario 3	17.0	15.9	16.6	15.8	-13.6	-11.1	-14.0	-13.1	-12.8	-12.4	-11.1	-10.8	-9.8	-10.0	-9.8	-9.1	-7.8	-9.6	-8.7	-10.0	11.0	11.1	10.3	11.1	12.0	12.3	13.7	16.5

A gamma distribution was selected to emulate the consumption of shiftable and controllable loads with DR potential. The parameters of the gamma distribution were determined from the actual data of each time zone, and the electricity consumption of each device was randomly generated through a random gamma function to which these parameters were applied. Fig. 12 presents a comparison between the actual and random values for the electricity consumption of the shiftable and controllable loads at the 12:30 time zone in home2. Similarly, for the entire dataset, values were selected for two months (Sep. and Oct.) and compared. Here, it was evident that the electricity consumption of each device appeared intermittently within the maximum value range. Moreover, the frequency of use was close to the actual value by reflecting the characteristics of each device.

Fig. 13 presents the results of changes in the consumption patterns of the total load, which were simulated according to the basic rules. As displayed in Fig. 13(a), the use of home appliances with DR potential shifted from the TOU time zone to the neighboring time zone. The electricity consumption before and after the TOU time zone increased by the shaded area, while electricity consumption during the TOU time zone decreased. In Fig. 13(b), each thin line represents the rate of change in electricity consumption in one iteration, and the bold line is a representative value for the potential of DR participation in home2. This was selected as the mean value of all iterations to mitigate the randomness of the results. As displayed in Table 3, each agent had different ownership characteristics of home appliances and electricity consumption over time; hence, the potential for DR participation was

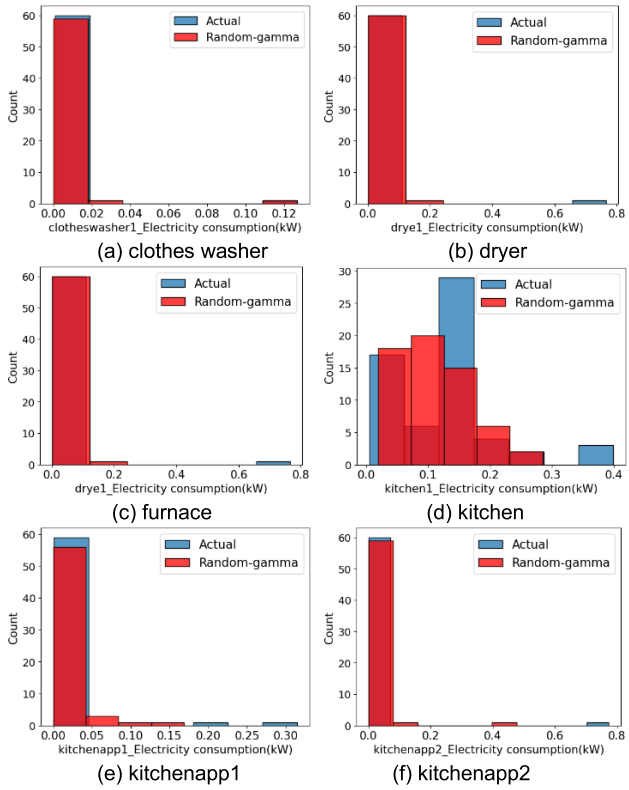

FIGURE 12. Comparison of actual and D-ABM values for each appliance's electricity consumption.

TABLE 6. Comparison of profit assuming deviations.

Bidding Strategy	Total profit ($)	Penalty cost ($)			
		Scenario 1	Scenario 2	Scenario 3	No DR
Scenario 1	258.89	-	16.46	20.18	15.51
Scenario 2	262.47	20.76	-	8.72	36.27
Scenario 3	263.87	27.01	11.26	-	42.52
Base Scenario (No DR)	238.59	-	-	-	-

also unique. For the sake of brevity, only the simulation process for home2 is presented herein, although the same process was applied to the other 10 consumer agents. The results of the potential for DR participation of all agents are displayed in Table 4.

C. BIDDING STRATEGY OF LOAD AGGREGATOR

The bidding strategy for maximizing the profit of the load aggregator (which is an intermediary) can be achieved by optimally determining the hourly bidding quantities without deviations in the day-ahead market. To reduce deviations, our study focused on deriving the DR participation rate to a more realistic value. In Table 4, the potential for each agent's participation in DR was estimated according to the agent's properties and the basic rules in D-ABM. However, the potential for DR participation at this time was close to the maximum value for participation.

Accordingly, D-ABM quantified the rate of change in total load due to participation in DR by additionally considering

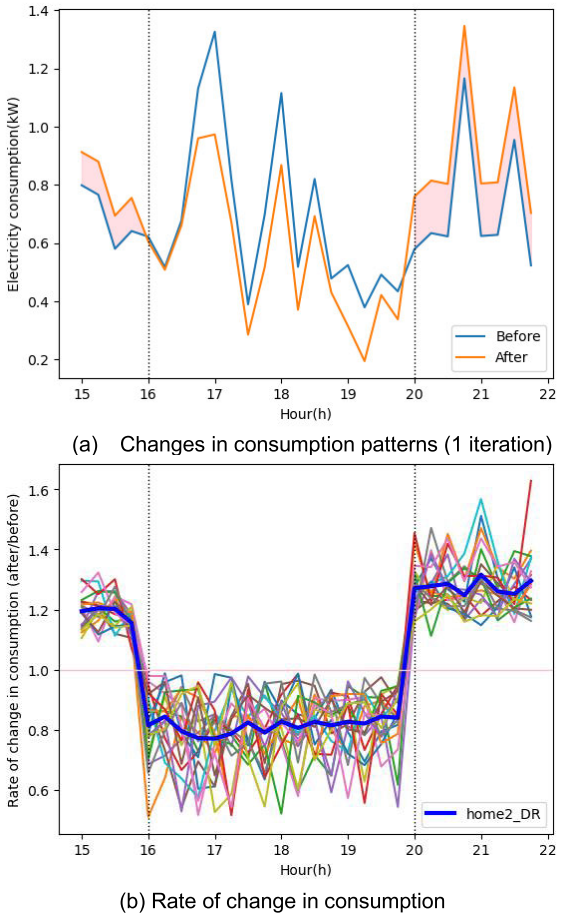

FIGURE 13. Changes in electricity consumption of home2 under TOU.

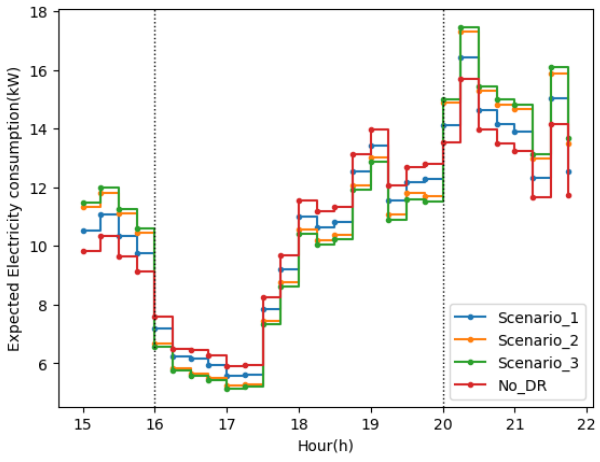

FIGURE 14. Estimated electricity consumption of the entire group by scenario.

several biases and preferences of each agent, which determined whether to participate in the DR program. The results were estimated by assuming three scenarios for the following biases and preferences that reflected the bounded rationality of consumers [6], [38], [39].

- Scenario 1 (endowment effect): People are relatively reluctant to trade because they value the things they own more highly. For example, a consumer may feel that they "own" the comfort. In this case, it was assumed that homes 1, 2, and 8, (which consumed less electricity during the TOU period yet had a high potential of participating in DR) did not participate due to inconvenience. For reference, the endowment effect can be perceived as a specific case of status quo bias.
- Scenario 2 (status quo bias): In a sociological sense, this is defined as a desire to maintain existing social structures or values. In other words, people tend to continue with the preset options, even when an alternative could produce better results. It was assumed that homes 6, 7, 9, and 10 were included. They consume a significant amount of electricity during the TOU period, but have a low DR potential, so they did not participate in DR due to low expected profit.
- Scenario 3 (pro-social preferences): Among the factors influencing energy consumption, appealing to pro-social preferences is more effective than buying DR. In this case, it was assumed that the entire group had a prosocial preference, which meant that each home cooperatively participated in the DR program with the maximum possible DR potential.

Table 5 presents the rates of change in the total load for each scenario. These were derived by considering the potential of DR participation in each time zone and the weight of an individual consumer's electricity consumption. In Scenario 1, the rate of change in total load over the TOU period was low (between -5.5% and $+7.2\%$) because no consumer with high DR potential participated. Scenario 3, where the maximum DR potential participated in DR, varied the rate of change in total load in the range of -14.0% to $+17\%$. The results for Scenario 2 had values close to Scenario 3 and exhibited a rate of change ranging from -12.9% to $+15.4\%$.

Fig. 14 depicts the expected electricity consumption obtained through the product of the change rate for each scenario and the total load value predicted by the data-driven forecasting model. Here, the predicted value of the aggregate load was selected as the value of 31 Oct. 2019, which was the day when no anomalies were detected. As demonstrated in Fig. 14, the rate of change in the total load for each scenario resulted in the load aggregator's various bidding strategies.

Table 6 displays a comparison of the total profit and penalty cost of the load aggregator considering possible deviations from the bidding strategy for each scenario. The total profit for all scenarios was higher compared to the base scenario without implementing the TOU tariff, with a difference of up to \$25. In the scenario-by-scenario comparison without deviations, Scenario 3 (where the DR participation rate was high) exhibited the highest profit. An analysis revealed that this was because (for Scenario 3) electricity consumption decreased the most during the period when the difference between the purchase price from the wholesale market and the retail price was small. Penalty costs appeared differently depending on the size of the deviations in each scenario. In the case of Scenario 1, assuming that the DR participation rate of Scenario 3 occurred, a penalty cost of \$20.18 was incurred for additional power sales and purchases in each time zone. Under this situation, the total revenue at this time reduced to a value similar to the base scenario. Similarly, in Scenario 3, if consumers did not participate in DR at all, the penalty cost of \$42.52 could result in a lower total profit than in the base scenario. These results suggested that an optimal bidding strategy was achieved by minimizing these deviations. Beyond the three scenarios, the strength of D-ABM was that as a bottom-up approach, various biases and preferences could be applied to each consumer agent individually. Since the overall simulation process of this study was based on data, if the bias and preference of each agent could be appropriately assigned through the analysis of historical or newly acquired data, a more realistic estimate of DR participation rates would be possible. Therefore, the proposed bidding strategy framework could create maximum profit for the load aggregator by reducing deviations when formulating a bidding strategy while considering the DR.

V. CONCLUSION

In this paper, a two-level optimal bidding strategy framework was proposed for load aggregators that combined a data-driven forecasting model and D-ABM to estimate the impact of DR in detail on electricity usage patterns. At the aggregated level, loads and market prices were predicted through an LSTM autoencoder-based forecasting model using multivariate time series data. Characterized by the reconstruction process, the LSTM autoencoders provided high forecasting performance and could be utilized for anomaly detection. At the individual level, the uncertainty of each consumer about the degree of DR participation was addressed through D-ABM. Moreover, the rate of change in total load was quantified under various assumptions about biases and preferences. By addressing uncertainties related to the bidding strategy at each level, our study focused on reducing deviations from the bidding strategy by estimating the change in total load under DR more realistically. In contrast to existing ABM studies in DR, this paper defined each consumer as a heterogeneous agent rather than only considering a single appliance or grouping consumer agents. Based on the actual individual data in each time zone, the properties of each agent were extracted through the statistical data analysis, and the random values generated by each consumer agent with these properties exhibited distribution and electricity consumption close to the actual values. Furthermore, as a bottom-up approach, D-ABM could more realistically estimate the extent to which total load changed under the influence of DR by assigning different biases and preferences to each consumer agent. It should be noted that the simulation results demonstrated that realistically estimating the impact

of total load under DR could minimize deviations from the bidding strategy, guaranteeing maximum profit. This work can be further improved by exploring bidding strategies for load aggregators participating in real-time markets and developing the proposed framework with a different price-based DR (e.g., real-time pricing) or incentive-based DR. Moving forward, the bidding strategies of load aggregators with various policies taken by the decision maker and bi-lateral contracts could also be investigated for practical applications in power systems.

REFERENCES

[1] L. Gkatzikis, I. Koutsopoulos, and T. Salonidis, "The role of aggregators in smart grid demand response markets," *IEEE J. Sel. Areas Commun.*, vol. 31, no. 7, pp. 1247–1257, Jul. 2013, doi: 10.1109/JSAC.2013.130708.

[2] A. A. Cook, G. Misirli, and Z. Fan, "Anomaly detection for IoT time-series data: A survey," *IEEE Internet Things J.*, vol. 7, no. 7, pp. 6481–6494, Jul. 2020, doi: 10.1109/JIOT.2019.2958185.

[3] F. Wang, B. Xiang, K. Li, X. Ge, H. Lu, J. Lai, and P. Dehghanian, "Smart households' aggregated capacity forecasting for load aggregators under incentive-based demand response programs," *IEEE Trans. Ind. Appl.*, vol. 56, no. 2, pp. 1086–1097, Mar. 2020, doi: 10.1109/TIA.2020.2966426.

[4] H. Socolow, *Saving Energy in the Home: Princeton's Experiment at Twin Rivers*. Philadelphia, PA, USA: Ballinger, 1978.

[5] Y. Wang, Q. Chen, T. Hong, and C. Kang, "Review of smart meter data analytics: Applications, methodologies, and challenges," *IEEE Trans. Smart Grid*, vol. 10, no. 3, pp. 3125–3148, May 2019, doi: 10.1109/TSG.2018.2818167.

[6] N. Good, "Using behavioural economic theory in modelling of demand response," *Appl. Energy*, vol. 239, pp. 107–116, Apr. 2019.

[7] O. Energy, "Blueprint for a post-carbon society: How residential flexibility is key to decarbonising power, heat and transport," Dept. Elect. Electron. Eng., Imperial College, London, U.K., Tech. Rep., 2018.

[8] H.-S. Ryu and M.-K. Kim, "Two-stage optimal microgrid operation with a risk-based hybrid demand response program considering uncertainty," *Energies*, vol. 13, no. 22, p. 6052, Nov. 2020, doi: 10.3390/en13226052.

[9] N. G. Paterakis, A. Tascikaraoglu, O. Erdinç, A. G. Bakirtzis, and J. P. S. Catalão, "Assessment of demand-response-driven load pattern elasticity using a combined approach for smart households," *IEEE Trans. Ind. Informat.*, vol. 12, no. 4, pp. 1529–1539, Aug. 2016, doi: 10.1109/TII.2016.2585122.

[10] Y. Chen, P. Xu, Y. Chu, W. Li, Y. Wu, L. Ni, Y. Bao, and K. Wang, "Short-term electrical load forecasting using the support vector regression (SVR) model to calculate the demand response baseline for office buildings," *Appl. Energy*, vol. 195, pp. 659–670, Jun. 2017, doi: 10.1016/j.apenergy.2017.03.034.

[11] X. Wang, Y. Wang, J. Wang, and D. Shi, "Residential customer baseline load estimation using stacked autoencoder with pseudo-load selection," *IEEE J. Sel. Areas Commun.*, vol. 38, no. 1, pp. 61–70, Jan. 2020, doi: 10.1109/JSAC.2019.2951932.

[12] D. Liu, Y. Sun, Y. Qu, B. Li, and Y. Xu, "Analysis and accurate prediction of user's response behavior in incentive-based demand response," *IEEE Access*, vol. 7, pp. 3170–3180, 2019, doi: 10.1109/ACCESS.2018.2889500.

[13] X. Kong, Z. Wang, F. Xiao, and L. Bai, "Power load forecasting method based on demand response deviation correction," *Int. J. Electr. Power Energy Syst.*, vol. 148, Jun. 2023, Art. no. 109013, doi: 10.1016/j.ijepes.2023.109013.

[14] S. Xu, X. Chen, J. Xie, S. Rahman, J. Wang, H. Hui, and T. Chen, "Agent-based modeling and simulation for the electricity market with residential demand response," *CSEE J. Power Energy Syst.*, vol. 7, no. 2, pp. 368–380, Mar. 2021, doi: 10.17775/CSEEJPES.2019.01750.

[15] K. Baek, E. Lee, and J. Kim, "Resident behavior detection model for environment responsive demand response," *IEEE Trans. Smart Grid*, vol. 12, no. 5, pp. 3980–3989, Sep. 2021, doi: 10.1109/TSG.2021.3074955.

[16] T. Wang, J. Wang, Y. Zhao, J. Shu, and J. Chen, "Multi-objective residential load dispatch based on comprehensive demand response potential and multi-dimensional user comfort," *Electr. Power Syst. Res.*, vol. 220, Jul. 2023, Art. no. 109331, doi: 10.1016/j.epsr.2023.109331.

[17] X. Yang, Z. Chen, X. Huang, R. Li, S. Xu, and C. Yang, "Robust capacity optimization methods for integrated energy systems considering demand response and thermal comfort," *Energy*, vol. 221, Apr. 2021, Art. no. 119727, doi: 10.1016/j.energy.2020.119727.

[18] F. Wang, X. Ge, K. Li, and Z. Mi, "Day-ahead market optimal bidding strategy and quantitative compensation mechanism design for load aggregator engaging demand response," *IEEE Trans. Ind. Appl.*, vol. 55, no. 6, pp. 5564–5573, Nov. 2019, doi: 10.1109/TIA.2019.2936183.

[19] H. J. Kim and M. K. Kim, "Risk-based hybrid energy management with developing bidding strategy and advanced demand response of grid-connected microgrid based on stochastic/information gap decision theory," *Int. J. Electr. Power Energy Syst.*, vol. 131, Oct. 2021, Art. no. 107046, doi: 10.1016/j.ijepes.2021.107046.

[20] S. Abapour, B. Mohammadi-Ivatloo, and M. T. Hagh, "Robust bidding strategy for demand response aggregators in electricity market based on game theory," *J. Cleaner Prod.*, vol. 243, Jan. 2020, Art. no. 118393, doi: 10.1016/j.jclepro.2019.118393.

[21] X. Liu, Y. Li, X. Lin, J. Guo, Y. Shi, and Y. Shen, "Dynamic bidding strategy for a demand response aggregator in the frequency regulation market," *Appl. Energy*, vol. 314, May 2022, Art. no. 118998, doi: 10.1016/j.apenergy.2022.118998.

[22] M. R. Mahmoudi, M. H. Heydari, S. N. Qasem, A. Mosavi, and S. S. Band, "Principal component analysis to study the relations between the spread rates of COVID-19 in high risks countries," *Alexandria Eng. J.*, vol. 60, no. 1, pp. 457–464, Feb. 2021, doi: 10.1016/j.aej.2020.09.013.

[23] S. Hochreiter and J. Schmidhuber, "Long short-term memory," *Neural Comput.*, vol. 9, no. 8, pp. 1735–1780, Nov. 1997, doi: 10.1162/neco.1997.9.8.1735.

[24] H. D. Nguyen, K. P. Tran, S. Thomassey, and M. Hamad, "Forecasting and anomaly detection approaches using LSTM and LSTM autoencoder techniques with the applications in supply chain management," *Int. J. Inf. Manage.*, vol. 57, Apr. 2021, Art. no. 102282, doi: 10.1016/j.ijinfomgt.2020.102282.

[25] C. Fan, F. Xiao, Y. Zhao, and J. Wang, "Analytical investigation of autoencoder-based methods for unsupervised anomaly detection in building energy data," *Appl. Energy*, vol. 211, pp. 1123–1135, Feb. 2018, doi: 10.1016/j.apenergy.2017.12.005.

[26] L. An, "Modeling human decisions in coupled human and natural systems: Review of agent-based models," *Ecological Model.*, vol. 229, pp. 25–36, Mar. 2012, doi: 10.1016/j.ecolmodel.2011.07.010.

[27] N. Gilbert, *Agent-Based Models*. Thousand Oaks, CA, USA: SAGE Publications, 2019.

[28] Y. Wang, H. Lin, Y. Liu, Q. Sun, and R. Wennersten, "Management of household electricity consumption under price-based demand response scheme," *J. Cleaner Prod.*, vol. 204, pp. 926–938, Dec. 2018, doi: 10.1016/j.jclepro.2018.09.019.

[29] G. Fagiolo, M. Guerini, F. Lamperti, A. Moneta and A. Roventini, "Validation of agent-based models in economics and finance," in *Computer Simulation Validation*. Cham, Switzerland: Springer, 2019, pp. 763–787.

[30] J. Osborne, "Improving your data transformations: Applying the Box-Cox transformation," *Practical Assessment, Res., Eval.*, vol. 15, no. 1, p. 12, 2010.

[31] X. He, N. Keyaerts, I. Azevedo, L. Meeus, L. Hancher, and J.-M. Glachant, "How to engage consumers in demand response: A contract perspective," *Utilities Policy*, vol. 27, pp. 108–122, Dec. 2013, doi: 10.1016/j.jup.2013.10.001.

[32] X. Lu, K. Li, H. Xu, F. Wang, Z. Zhou, and Y. Zhang, "Fundamentals and business model for resource aggregator of demand response in electricity markets," *Energy*, vol. 204, Aug. 2020, Art. no. 117885, doi: 10.1016/j.energy.2020.117885.

[33] R. H. Thaler, "Mental accounting matters," *J. Behav. Decis. Making*, vol. 12, no. 3, pp. 183–206, Sep. 1999.

[34] F. Wang, X. Ge, P. Yang, K. Li, Z. Mi, P. Siano, and N. Duić, "Day-ahead optimal bidding and scheduling strategies for DER aggregator considering responsive uncertainty under real-time pricing," *Energy*, vol. 213, Dec. 2020, Art. no. 118765, doi: 10.1016/j.energy.2020.118765.

[35] *Pecan Street Dataport*. Accessed: Nov. 29, 2022. [Online]. Available: https://www.pecanstreet.org/dataport/

[36] New York Independent System Operator. Accessed: Dec. 23, 2022. [Online]. Available: https://www.nyiso.com/energy-market-operational-data

[37] H. J. Kim, H. J. Kang, and M. K. Kim, "Data-driven bidding strategy for DER aggregator based on gated recurrent unit-enhanced learning particle swarm optimization," *IEEE Access*, vol. 9, pp. 66420–66435, 2021, doi: 10.1109/ACCESS.2021.3076679.

[38] N. Camara, D. Xu, and E. Binyet, "Understanding household energy use, decision making and behaviour in Guinea-Conakry by applying behavioural economics," *Renew. Sustain. Energy Rev.*, vol. 79, pp. 1380–1391, Nov. 2017, doi: 10.1016/j.rser.2017.03.128.

[39] J. Bruner, F. Calegari, and T. Handfield, "The evolution of the endowment effect," *Evol. Human Behav.*, vol. 41, no. 1, pp. 87–95, Jan. 2020, doi: 10.1016/j.evolhumbehav.2019.10.004.

HAN SEOK RYU received the B.S. degree from the Department of Physics, Yeung-Nam University, Gyeongsan, South Korea, in 2007, and the M.S. degree from the Department of Energy System Engineering, Chung-Ang University, Seoul, South Korea, in 2023. His research interests include microgrids, demand response, and agent-based modeling.

HYUNG JOON KIM received the B.S. and M.S. degrees from the Department of Energy System Engineering, Chung-Ang University, Seoul, South Korea, in 2018 and 2021, respectively, where he is currently pursuing the Ph.D. degree. His research interests include data-driven modeling, machine-learning in smart grid, power system data analysis, forecasting, microgrids, demand response, and energy management systems.

MUN KYEOM KIM received the Ph.D. degree from the School of Electrical and Computer Engineering, Seoul National University. He is currently a Professor with the School of Energy System Engineering, Chung-Ang University, Seoul, South Korea. His research interests include the operation techniques in hybrid AC/DC power systems, AI-based smart power networks, big data-based demand response, real-time market design, and multi-agent-based smart city intelligence.